7. Kinetic Study of the Reactions between $[MnN(H_2O)(CN)_4]^{2-}$ and Different Mono- and Bidentate Ligands.

7.1. Introduction

Kinetic studies over the past few years have shown that the aquanitridotetracyano complexes of technetium(V), rhenium(V) and osmium(VI) can undergo anation reactions with monodentate ligands like CN^- and N_3^-.[1,2] These kinetic studies have also shown that the aqua complexes can be deprotonated to form the hydroxo complexes and that these are inert towards substitution reactions (see § 2.2).

The analogous *trans*-dioxotetracyano complexes of molybdenum(IV), tungsten(IV), technetium(V) and rhenium(V) can be protonated as well, resulting in the formation of the oxohydroxo- and oxoaqua complexes (see § 2.1).[3,4,5,6,7] These protonated species can undergo substitution reactions with mono- (aqua ligand substitution)[8,9,10,11,12,13,14] and bidentate (aqua and cyano ligand substitution)[15,16,17] nucleophiles. The protonation behaviour as well as the cyanide exchange of these systems has recently been the subject of carbon-13 and oxygen-17 NMR studies in

[1] Damoense, L.J.; Purcell, W.; Leipoldt, J.G., *Transition Met. Chem.*, **1994**, *19*, 619.
[2] Van der Westhuizen, H.J.; Basson, S.S.; Leipoldt, J.G; Purcell, W., *Polyhedron*, **1994**, *13*, 717.
[3] Robinson, P.R.; Schlemper, E.O.; Murmann, R.K., *Inorg. Chem.*, **1975**, *14*, 2035.
[4] Heijmo, E.; Kanas, A.; Samotus, A., *Bull. Acad. Polon. Sci. Ser. Sci. Chim.*, **1973**, *21*, 311.
[5] Roodt, A.; Leipoldt, J.G.; Deutsch, E.A.; Sullivan, J.C., *Inorg. Chem.*, **1992**, *31*, 1080.
[6] Chakravorti, M.C., *J. Inorg. Nucl. Chem.*, **1972**, *34*, 893.
[7] Purcell, W.; Roodt, A.; Basson, S.S.; Leipoldt, J.G., *Transition Met. Chem.*, **1991**, *16*, 60.
[8] Potgieter, I.M.; Basson, S.S.; Roodt, A, ; Leipoldt, J.G., *Transition Met. Chem.*, **1988**, *13*, 209.
[9] Smit, J.P.; Purcell, W.; Roodt, A.; Leipoldt, J.G., *Polyhedron*, **1993**, *12*, 2271.
[10] Smit, J.P.; *Ph.D. thesis*, University of the Free State, Bloemfontein, South Africa, **1995**.
[11] Leipoldt, J.G.; Van Eldik, R.; Basson, S.S.; Roodt, A., *Inorg.Chem.*, **1986**, *25*, 4639.
[12] Roodt, A.; Leipoldt, J.G.; Basson, S.S.; Potgieter, I.M., *Transition Met. Chem.*, **1988**, *13*, 336.
[13] Purcell, W.; Roodt, A.; Basson, S.S.; Leipoldt, J.G., *Transition Met. Chem.*, **1989**, *14*, 224.
[14] Purcell, W.; Roodt, A.; Leipoldt, J.G., *Transition Met. Chem.*, **1991**, *16*, 339.
[15] Leipoldt, J.G.; Basson, S.S.; Potgieter, I.M.; Roodt, A, *Inorg.Chem.*, **1987**, *26*, 57.
[16] Samotus, A.; Kanas, A.; Glug, W.; Szklarzewicz, J., *Transition Met. Chem.*, **1991**, *16*, 614.

order to investigate the water and cyanide exchange of these complexes.[18]

Previous studies of the substitution reactions of these oxoaqua complexes included different monodentate nucleophiles such as F^-, N_3^-, NCS^-, pyridine (py) and substituted thioureas for the tungsten(IV) and rhenium(V) complexes.[10,11,12,13,14] Only reactions of the F and CN^-/HCN ions with the molybdenum(IV) complex could be studied due to the high lability of the coordinated aqua ligand in the $[MoO(H_2O)(CN)_4]^{2-}$ complex.[8,9] Thus, it was impossible to do extensive kinetic studies, specifically high pressure studies, on the substitution reactions of the $[MoO(H_2O)(CN)_4]^{2-}$ complex. The kinetic study of the monodentate substitution (N_3^-, NCS^-, py) of the aqua ligand of the $[WO(H_2O)(CN)_4]^{2-}$ complex showed that a linear free energy relationship between $\ln k_L$ and $\ln K_L$ (k_L is the hydrolysis rate constant and K_L is the stability constant for the $[WO(L)(CN)_4]^{n-}$) exists and the existence of this relationship points towards a dissociative mechanism for these substitution reactions. Even more convincing evidence for a dissociative mechanism for these type of substitution reactions was the observed positive volume of activation [+10.5(5) cm^3 mol^{-1}] for the reaction between $[WO(H_2O)(CN)_4]^{2-}$ and N_3^- anions.[12]

The above-mentioned complexes can also undergo substitution by bidentate ligands. The crystal structure determinations of the products[19,20,21] of the reactions between the oxoaqua complexes and bidentate ligands showed that the aqua ligand and one of the cyano ligands in the equatorial plane are substituted by the entering bidentate nucleophiles. It is expected that the aqua ligand will be substituted first during the two step process, since the metal-aqua bond is usually much weaker than a metal-cyano bond in this type of complexes, especially as a result of the large *trans* influence of the oxo ligand. The crystal structure determination of the $[WO(pic)(CN)_4]^{2-}$ complex[21] (pic = pyridine-2-carboxylate) showed that an oxygen atom of the carboxylic group is bonded *trans* to the nitrido ligand and that the nitrogen atom is bonded *trans* to a cyano ligand in the equatorial plane of the octahedral complex. This is interpreted to mean that the aqua ligand is indeed

[17] Roodt, A.; Basson, S.S.; Leipoldt, J.G., *Polyhedron*, **1994**, *13*, 599.
[18] Roodt, A.; Leipoldt, J.G.; Helm, L.; Abou-Hamdan, A.; Merbach, A.E., *Inorg.Chem.*, **1995**, *34*, 560.
[19] Basson, S.S.; Leipoldt, J.G.; Potgieter, I.M., *Inorg. Chim. Acta*, **1984**, *87*, 71.
[20] Szklarzewicz, J.; Samotus, A.; Alcock, N.W.; Moll, M., *J. Chem. Soc., Dalton Trans.*, **1990**, 2959.

substituted first, since it is known that the oxygen atom of the carboxylic ligand will bond before the nitrogen atom in this type of bidentate ligand. The substitution reactions of the $[WO(H_2O)(CN)_4]^{2-}$ complex with monodentate ligands are about a 1000 times faster compared to the bidentate substitution reactions as well as the fact that the above-mentioned kinetic evidence shows that a dissociative mechanism is operative, gives a strong indication that the substitution of the aqua ligand is the fast first reaction.[10,11,12] The substitution of the cyano ligand and the simultaneous ring-closure of the chelate ring is a relatively slow reaction and this reaction is the rate determining step in the overall process.[17]

The above-mentioned reactions of the corresponding manganese(V) complexes have also been complimented by crystallographic studies on the $[MnN(pic)(CN)_3]^{2-}$ and $[MnN(quin)(CN)_3]^{2-}$ complexes (see Chapter 6). In both these structures the oxygen atom of the carboxylic group is bonded *trans* to the nitrido ligand and the nitrogen atom of the pyridine ring is bonded *trans* to one of the equatorial cyano ligands. Thus, it was important to study this system and determine the reaction rates for both the monodentate and bidentate substitution reactions of the $[MnN(H_2O)(CN)_4]^{2-}$ complex to establish if these substitution reactions proceed *via* a dissociative mechanism.

7.2. Chemicals and Instrumentation

Caution! Cyanide compounds are extremely toxic and HCN can be generated under certain conditions while working with these compounds. Therefore, the appropriate care must be taken as far as possible, *e.g.*, to perform all manipulations in an efficient fume hood.

The substitution reactions of the $[MnN(H_2O)(CN)_4]^{2-}$ complex and the following four pyridine carboxylate ligands, i.e. pyridine-2-carboxylate (pic^-), pyridine-2,3-dicarboxylate ($2,3\text{-dipic}^{2-}$), pyridine-2,4-dicarboxylate ($2,4\text{-dipic}^{2-}$) and pyridine-2,5-dicarboxylate ($2,5\text{-dipic}^{2-}$) were studied during the course of this kinetic study. No

[21] Leipoldt, J.G.; Basson, S.S.;Roodt, A.; Potgieter, I.M., *Transition Met. Chem.*, **1986**, *11*, 323.

reaction was observed between $[MnN(H_2O)(CN)_4]^{2-}$ and pyridine-2,6-dicarboxylate (2,6-dipic^{2-}) and this might be ascribed to the steric interaction between the second carboxylate moiety in the 6-position of the pyridine ring and the nitrido ligand of the complex. The substitution reaction of $[MnN(H_2O)(CN)_4]^{2-}$ with quinaldinate (quin$^-$) could not be studied by means of spectrophotometry, since very small absorbance changes were observed for this reaction. The reactions of $[MnN(H_2O)(CN)_4]^{2-}$ with 1,10-phenanthroline (phen) and 2,2'-bipyridine (2,2'-bipy) could not be studied due to the low solubility of these bidentate ligands in aqueous medium. However, it was not deemed important at this stage to study the reaction of $[MnN(H_2O)(CN)_4]^{2-}$ with ethylenediamine (en), since the reactions of the aqua complex with 1,10-phenanthroline and 2,2'-bipyridine could not be studied.

Table 7.1: Acid dissociation constants for the pyridine carboxylate type ligands.

Pyridine carboxylic acids	pK_{a1} [a]	pK_{a2} [b]	Ref.
Pyridine-2-carboxylic acid	1.03	5.02	[22]
Pyridine-2,3-dicarboxlic acid	2.78	5.02	[23]
Pyridine-2,4-dicarboxlic acid	2.17	5.09	[24]
Pyridine-2,5-dicarboxlic acid	2.31	5.06	[24]
Pyridine-2,6-dicarboxlic acid	-0.81	4.97	[25]
Quinoline-2-carboxylic acid	1.9	4.97	[26]

[a] Dissociating group = -COOH

[b] Dissociating group = $-NH^+$

All experiments were carried out under aerobic conditions and double distilled water was used in all the preparations unless otherwise mentioned. All chemicals used in these kinetic studies were purchased from either Merck or Sigma-Aldrich Chemical Company. The chemicals were of analytical grade or better and were used without any further purification. The reactant and product complexes were synthesized as reported earlier (§ 3.3 and Chapter 6). All solutions of the respective complexes and

[22] Garcia, B.; Ibeas, S.; Leal, J.M., *J. Phys. Org. Chem.,* **1996**, *9*, 593.
[23] Harmon, K.M.; Brown, P.W.; Gill, S.H., *J. Mol. Struct*., **1998**, *448*, 43.
[24] Canic, G.; *Glas. Hem. Drus. Beograd.*; **1955**, *29*, 35.
[25] Tichane, S.; Bennett, T., *J. Am. Chem. Soc.*; **1957**, *79*, 1293.
[26] Martell, A.E.; Smith, R.M., *Critical Stability Constants*, Plenum Press, **1982**, 129.

ligands were prepared immediately before use. All the kinetic runs were performed under pseudo first-order conditions in a carbonate/hydrogen carbonate buffer medium with the ionic strength adjusted to μ = 1.0 M using KNO_3. No reaction between KNO_3 and $[MnN(H_2O)(CN)_4]^{2-}$ could be detected.

All pH measurements were recorded on a Hanna pH211 bench-top pH meter equipped with a HI1043B refillable combination glass pH electrode using standard buffer solutions for calibration. The filling solution of the electrode was also replaced on a daily basis before each calibration and subsequent measurements. In all calculations pH = -log $[H^+]$.

The UV/visible spectral and absorbance changes for the fast kinetic reactions were measured on a Hi Tech SF61DX2 Stopped Flow System with a thermostatted SHU61DX sample handling unit and an attached Jalabu MPV thermostatted water bath (accurate within $\pm$ 0.05 °C). The rate constants were determined using the KinetAsyst 3.10[27] software package supplied with the stopped-flow instrument. The UV/Vis spectral and absorbance changes for the slow kinetic reactions were measured on Varian Cary 50 Conc and Varian 100 spectrophotometers with 1.000 $\pm$ 0.001 cm path length tandem quartz cells. All the spectrophotometers were equipped with constant temperature cell holders (accurate within 0.1 °C) and Jalabu MPV thermostatted water baths (accurate within 0.05 °C) fitted with circulators and all the temperatures are reported to $\pm$ 0.1 °C accuracy. The spectrophotometers were coupled with personal computers capable of performing least-squares analyses (Scientist)[28] on the absorption *vs.* time data obtained from the kinetics runs and the spectral changes, respectively. The solid lines in the Figures represent the least-squares computer fits of the experimental data to the respective functions. Complete tables of k_{obs} *vs.* [L], k_{obs} *vs.* pH and absorbance *vs.* [L] data used for the particular figures presented in the next section are given as supplementary data in Appendix C.

[27] KinetAsyst 3.10 Software Package, Hi-Tech Limited, Salisbury, United Kingdom, **2002**.
[28] MicroMath Scientist for Windows, Version 2.01, MicroMath Inc., **1995**.

7.3. Results of the monodentate substitution reactions of the $[MnN(H_2O)(CN)_4]^{2-}$ complex.

Previous research has shown that the $[MN(H_2O)(CN)_4]^{n-}$ complex [M = rhenium(V) and osmium(VI)] is the only complex of the nitridotetracyano complexes which is reactive towards substitution reactions and that the hydroxo ligand in $[MN(OH)(CN)]^{(n+1)-}$ is not substituted by entering nucleophiles, *i.e.*, the hydroxo complex is inert towards substitution reactions.[1,2] These observations enabled the construction of the reaction scheme as represented by Scheme 7.1 for the substitution reactions with monodentate nucleophiles as well as the deprotonation reactions of the $[M(H_2O)(CN)_4]^{n-}$ complexes in solution.

The starting compounds of the nitridotetracyano of the rhenium(V) and osmium(VI) analogues were the aqua complexes and these were reacted with the entering nucleophiles.[1,2] However, the starting compound for the reactions of the nitridotetracyano complexes of manganese(V) is $[(CH_3)N]_2Na[MnN(CN)_5]\cdot H_2O$. The *trans* bonded cyano ligand dissociates in solution to form the aqua complex (reaction **A**, Scheme 7.1) and the aqua complex react with other monodentate or even bidentate nucleophiles to form the desired substitution products. The crystal structures of the $[MnN(NCS)(CN)_4]^{3-}$ and $[MnN(pic)(CN)_3]^{2-}$ complexes as well as the synthesis of the $[MnN(N_3)(CN)_4]^{3-}$ complex support this observation (see Paragraph 3.3.8, Chapter 4 and 6). Thus, the following reaction scheme (Scheme 7.1) can be constructed to depict the behaviour of the $[MnN(CN)_5]^{3-}$ complex in solution.

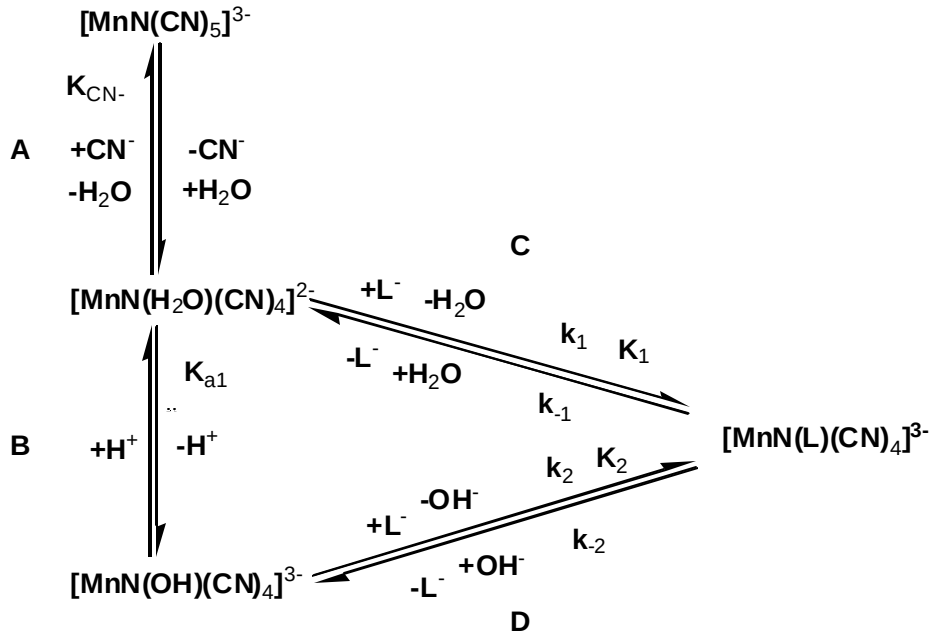

Scheme 7.1: The dissociation and solution behaviour of the $[MnN(CN)_5]^{3-}$ complex in aqueous medium.

Unfortunately, the acid dissociation constant (pK_{a1}) of the aqua complex could not be determined due to the relatively small difference in the UV/visible absorbance spectra of the aqua and hydroxo complexes (see reaction **B**, Scheme 7.1). However, results from the kinetic studies of the monodentate substitution reactions of the $[MN(H_2O)(CN)_4]^{n-}$ complexes [M = rhenium and osmium(VI)] have shown that the hydroxo complexes do not react with monodentate nucleophiles.[1,2] Thus, the numerical value of the forward reaction between the $[MN(OH)(CN)_4]^{3-}$ and monodentate ligands (k_2) is taken to be zero within experimental error (reaction **D**, Scheme 7.1). The same tendency is expected for the substitution reactions of the $[MnN(OH)(CN)]^{3-}$ with monodentate nucleophiles as well.

The UV/visible spectrum of the reaction between $[MnN(H_2O)(CN)_4]^{2-}$ and added CN^- ions showed only one maximum in the spectrum at 285 nm. In the spectrophotometric determination of the stability constant of the $[MnN(CN)_5]^{3-}$ complex the concentration of the CN^- was varied from 0.005 M to 0.10 M. The plot of absorbance *vs.* the concentration of the entering ligand (Figure 7.1) revealed that under the experimental conditions $[MnN(H_2O)(CN)_4]^{2-}$ reacts with CN^- in a 1:1 ratio

and that it is in agreement with the structure determination of $[MnN(CN)_5]^{3-}$.[29] The equilibrium constant for the reaction between $[MnN(H_2O)(CN)_4]^{2-}$ and CN^- was determined by a least-squares fit of the absorbance *vs.* cyanide concentration to eq. 7.1 and is shown in Figure 7.1. The equation is derived from Beer's law, the mass balance equation and the definition of the stability constant, K_1, for the reaction **A** in Scheme 7.1 (see Appendix B.2). The stability constant for the $[MnN(CN)_5]^{3-}$ complex was determined as 168(20) M^{-1}.

$$A_{obs} = \frac{A_M + A_{ML}K_1[CN^-]}{1 + K_1[CN^-]} \qquad 7.1$$

In eq. 7.1 A_M and A_{ML} represents the absorbance of the $[MnN(H_2O)(CN)_4]^{2-}$ and $[MnN(CN)_5]^{3-}$ complexes, A_{obs} the observed absorbance and K_1 the equilibrium constant of the reaction, respectively.

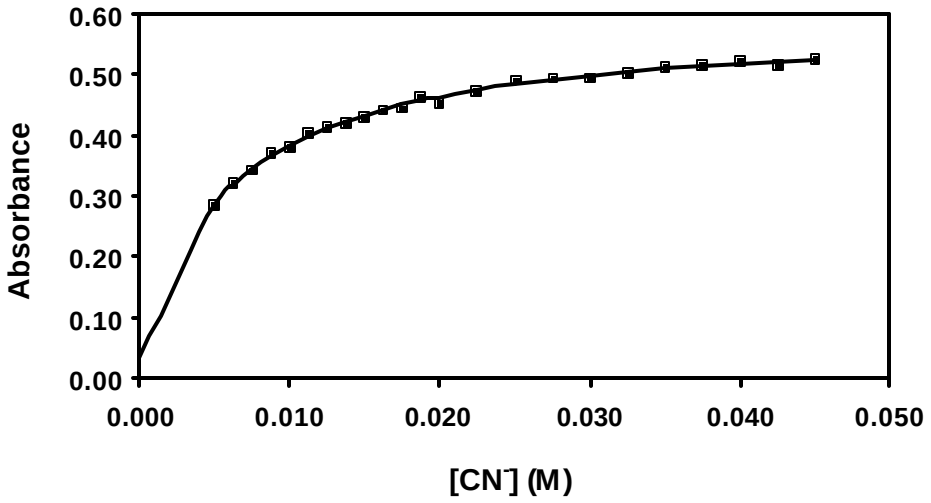

Figure 7.1: Plot of absorbance *vs.* $[CN^-]$ at 25.2 °C, $[MnN]_T = 5.05 \times 10^{-4}$ M, μ = 1.0 M (NaCl), pH 11.01 and ? = 285 nm.

The forward reactions of the $[MnN(H_2O)(CN)_4]^{2-}$ with monodentate ligands (CN^-, NCS^- and N_3^-) were very fast; in fact, so fast that the reaction rates of the substitution reactions could not be determined on a 3rd generation stopped-flow spectrophotometer. This spectrophotometer has a mixing time of ± 1 ms before the

[29] Bendix, J.; Deeth, R.J.; Weyherm üller, T.; Bill, E.; Wieghardt, K., *Inorg.Chem.*, **2000**, *39*, 930.

measurement of the absorbance *vs.* time data starts, which means that these reactions were complete within 1 ms. If the standard equation for the calculation of the half-life of the pseudo first-order reaction is used, a value of larger than 1000 s^{-1} is obtained for the observed rate constant, k_{obs}, at $[CN^-]$ = 0.05 M. If the forward rate constant is calculated using the minimum value of the observed rate constant and the concentration of the entering ligand, a value of $k_1 > 20000$ M^{-1} s^{-1} is obtained, which indicates that the substitution reactions of the $[MnN(H_2O)(CN)_4]^{2-}$ complex are extremely fast. The same results concerning the forward rate of the substitution reactions of the $[MnN(H_2O)(CN)_4]^{2-}$ complex were obtained with other entering ligands, *i.e.*, NCS^- and N_3^-. However, since the stability constants for the known monodentate substituted $[MO(L)(CN)_4]^{n-}$ complexes, L = CN^-, F^-, N_3^-, NCS^- ions and py, are for the molybdenum(IV) complexes: 95(5), 12.1(9), 1.5(1), 0.2(1), 0.05(2) M^{-1} and for the tungsten(IV) complexes: 1.1(1) x 10^3, 1.4(2) x 10^2, 4.8(11), 2.0(1), 0.5(1) M^{-1}, it is expected that the stability constants (reaction **C**, Scheme 7.1) for the $[MnN(NCS)(CN)_4]^{3-}$ and $[MnN(N_3)(CN)_4]^{3-}$ complexes will be much smaller compared the stability constant of the $[MnN(CN)_5]^{3-}$ complex [K_1 = 168(20) M^{-1}].

7.4. Results of the bidentate substitution reactions of the $[MnN(H_2O)(CN)_4]^{2-}$ complex.

The crystal structure determinations of both the $(Ph_4As)_2[MnN(pic)(CN)_3]\cdot 4H_2O$ and $(Ph_4As)_2[MnN(quin)(CN)_3]\cdot 3H_2O$ complexes showed that, in both final products from the reactions of $[MnN(H_2O)(CN)_4]^{2-}$ with pic^- and $quin^-$ anions respectively, the pyridine carboxylate type ligands coordinate to the manganese(V) metal center with the oxygen atom of the carboxylate group *trans* to the nitrido ligand and that the pyridine nitrogen atom substituted an equatorial cyano ligand. The following reaction scheme may be constructed for describing the substitution process of the aqua and cyano ligands in $[MnN(H_2O)(CN)_4]^{2-}$ with bidentate ligands (Scheme 7.2).

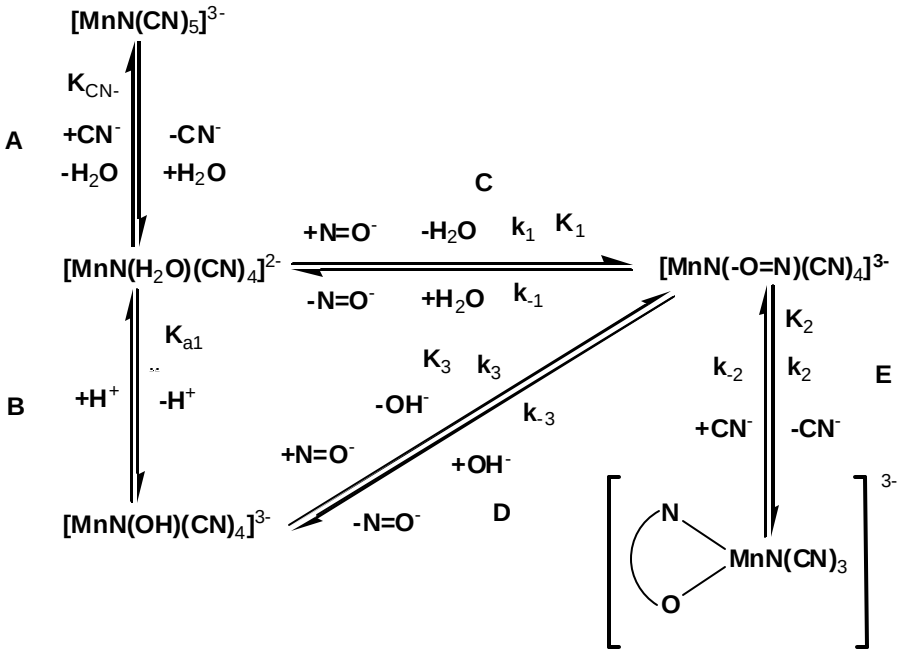

Scheme 7.2: The protonation and bidentate substitution behaviour of the $[MnN(H_2O)(CN)_4]^{2-}$ complex (N=O = picolinate type ligands).

The results of the crystal structure determination of the $[MnN(pic)(CN)_3]^{2-}$ complex showed that in Scheme 7.2 the first step (reaction **C**) is the substitution of the aqua ligand by the oxygen atom of the carboxylate group (k_1 path) with the formation of the $[MnN(\eta^1\text{-pic})(CN)_4]^{3-}$ complex. This is followed by the substitution of the cyano ligand by the nitrogen atom of the pyridine moiety (ring closure of the chelate) during the second step (k_2 path, reaction **E**) and the resultant formation of the $[MnN(\eta^2\text{-pic})(CN)_4]^{2-}$ complex. It was estimated that the equilibrium constant, K_1, for the aqua substitution by the carboxylate moiety of pic^- is quite small, since the equilibrium constant, K_1, that was obtained for the reaction between $[WO(H_2O)(CN)_4]^{2-}$ and pic^- [$K_1 = 1.1(2)\ M^{-1}$][17] was relatively small. The equilibrium constant, K_1, reported for the reaction between $[MoO(H_2O)(CN)_4]^{2-}$ and phen [$K_1 = 5.6(3) \times 10^2\ M^{-1}$][15] is actually the overall equilibrium constant, since only one reaction was observed and it was thought that aqua substitution is the rate-determining step of the two-step process. A larger value was obtained for the overall equilibrium constant of the tungsten(IV) system [$K' = 13(2)\ M^{-1}$] than the equilibrium constant of the aqua substitution, which might also indicate that the K_1-value reported for the molybdenum(IV) system is the overall equilibrium constant (K').

7.4.1. Determination of the rate laws

The rate equation from Scheme 7.2 may have different forms depending on the rate determining step, i.e., aqua/hydroxo substitution or CN^- substitution and ring-closure. The total reaction was interpreted in terms of the two rate determining steps ($k_1 + k_3$ and k_2) in Scheme 7.2. The pseudo first-order rate constant, where $[pic^-] >> [manganese(V)]$, for the substitution of the aqua/hydroxo ligand and the formation of the $[MnN(\eta^1\text{-pic})(CN)_4]^{3-}$ complex in the first step (reaction **C**) in Scheme 7.2 is given by eq 7.2. This equation is similar to the rate equation derived for monodentate substitution reactions of the $[MN(H_2O)(CN)_4]^{n-}$ complexes [M = rhenium(V) and osmium(VI)][1,2] (see Appendix B.3).

$$k_{obs} = \frac{k_1 + k_3(K_{a1}/[H^+])[pic^-]}{1 + K_{a1}/[H^+]} + k_{-1} + k_{-3}[OH^-] \qquad 7.2$$

The second ring-closing step or the k_2 path (reaction **E**, Scheme 7.2; substitution of the cyano ligand) is much slower than the first aqua substitution step or the k_1 path in Scheme 7.2 and the rate equation for the formation of the final $[MnN(\eta^2\text{-pic})(CN)_3]^{2-}$ complex can be described by eq. 7.3. This assumption was made due to the fact that the rates of the monodentate substitution reactions of the $[MnN(H_2O)(CN)_4]^{2-}$ complex were too fast to be determined (see Section 7.3) and from results obtained from a kinetic study of the reaction between $[WO(H_2O)(CN)_4]^{2-}$ and pic^-.[17] Two distinct reactions were observed for the substitution of the aqua- and cyano ligands during the reaction of the $[WO(H_2O)(CN)_4]^{2-}$ complex with pic^- anions.[17] The rate of first reaction was very fast compared to slower rate of the second reaction and this was interpreted as the substitution of the aqua ligand being very fast compared to the rate of substitution of the cyano ligand. This is also in accordance to the monodentate substitution behaviour of the $[MN(H_2O)(CN)_4]^{n-}$/$[MO(H_2O)(CN)_4]^{n-}$ [MN = rhenium(V), osmium(VI) and MO = molybdenum(IV), tungsten(IV), technetium(V) and rhenium(V)][1,2,8,9,10,11,12,13,14] complexes where only the aqua ligand is substituted and none of the equatorial cyano ligands. The contribution of the reverse reaction or the uptake of the cyanide anion during the reaction is represented by the term k'_{-2}.

$$k_{obs} = \frac{k_2K_1[pic^-]}{1 + K_{a1}/[H^+] + K_1[pic^-]} + k'_{-2} \qquad 7.3$$

Equation 7.3[17] assumes that the hydroxo complex is inert towards substitution, i.e. $k_3 << k_1$, and the fact that these reaction were carried out at a pH-value where the aqua complex is the dominant species in solution (pH = 10.00). It was found during kinetic studies of the monodentate substitution reactions of the $[MN(H_2O)(CN)_4]^-$ complexes [M = rhenium(V) and osmium(VI)][1,2] that the hydroxo complexes are inert towards substitution reactions with monodentate ligands. If linear plots are obtained for the pseudo first-order constants (k_{obs}) *vs.* [pic$^-$] data, then eq. 7.3 can be simplified to eq. 7.4.

$$\mathbf{k_{obs} = \frac{k_2 K_1 [pic^-]}{1 + K_{a1}/[H^+]} + k'_{-2}} \qquad \mathbf{7.4}$$

Furthermore, at pH values of *ca.* 10.0 ($K_{a1} << [H^+]$), eq. 7.4 can be simplified to eq. 7.5.

$$\mathbf{k_{obs} = k_2 K_1 [pic^-] + k'_{-2}} \qquad \mathbf{7.5}$$

Unfortunately, since the first reactions between $[MnN(H_2O)(CN)_4]^{2-}$ and the different pyridine carboxylate ligands were too fast to be studied and the fact that the absorbance *vs.* time data for the slow reaction showed only one reaction at the chosen wavelength, the value of K_1 could not be determined and eq. 7.5 can be rewritten as given in eq. 7.6; however, all the kinetic evidence points to small K_1 values.

$$\mathbf{k_{obs} = k'_1 [pic^-] + k'_{-1}} \qquad \mathbf{7.6}$$

The value of k'_1 is the product of the forward rate constant for the slow second ring closure reaction (k_2, reaction **E**) and the equilibrium constant of the first reaction (K_1, reaction **C**), and k'_{-1} represents the contribution of the reverse reaction of the uptake (k'_{-2}) of the cyanide anions. The values for k'_1 and k_{-1} were obtained from the slope and the intercept, respectively, by means of the least-squares fit of the k_{obs} *vs.* [pic$^-$] data to eq. 7.6. Only the data for the three lower temperature values are shown in the plots of k_{obs} *vs.* [pic$^-$] for the reactions of $[MnN(H_2O)(CN)_4]^{2-}$ with the different pyridine carboxylate type ligands, but the different rates (k_1) for the reactions were

measured at least at five different temperatures. This was done to obtain more data for a more accurate determination of the activation parameters.

At pH values of *ca.* 14, $[H^+] << K_{a1}$, eq. 7.2 can be simplified to eq. 7.7.

$$k_{obs} = \frac{k'_1 + k'_2 (K_{a1}/[H^+])[pic^-]}{1 + K_{a1}/[H^+]} + k'_{-1} + k'_{-2}[OH^-] \qquad 7.7$$

The pH dependence of the pseudo first-order rate constant for the second slow reaction is illustrated in Figure 7.4 (example). The data in Figure 7.4 were fitted to eq. 7.7 with k'_1 the rate constant for the overall reaction determined at low pH values and k'_2 the rate constant determined for the overall reaction determined at high pH values. The terms k'_{-1} and k'_{-2} describe the reverse reactions at low and high pH values for the overall process.

Attempts were also made to determine the rate of the overall reaction (k'_2) at high pH, but the results obtained were dubious, since it was found that the products obtained by the reactions of $[MnN(H_2O)(CN)_4]^{2-}$ with different pyridine carboxylates decomposed at high pH. The absorbance changes of these decomposition reactions were in the region where the absorbance changes took place for the substitution reactions and therefore accurate rate constants could not be determined.

The temperature dependencies for the second step were used to calculate the activation parameters for the overall process of the bidentate substitution reactions of the $[MnN(H_2O)(CN)_4]^{2-}$ complex using the Eyring equation (eq. 7.8, see Appendix B.4) and the values are reported in Table 7.2.

$$\ln\frac{k}{T} = \ln\frac{k_B}{h} + \frac{\Delta S^{\neq}}{R} - \frac{\Delta H^{\neq}}{RT} \qquad 7.8$$

In eq. 7.8 k_B is the Boltzman constant, h is the Planck constant, R is the gas constant, $\Delta S^{?}$ and $\Delta H^{?}$ are the entropy and enthalpy of activation respectively. More complete derivations for eq. 7.2 and 7.8 as well as some general kinetic considerations are given in the supplementary material (Appendix B).

7.4.2. Reaction with pyridine-2-carboxylate (pic^-)

The UV/visible spectrum of the reaction between $[MnN(H_2O)(CN)_4]^{2-}$ and pyridine-2-carboxylate (pic^-) anions showed only one maximum at 350 nm. The stability constant (K′, Table 7.2) for the overall reaction between the $[MnN(H_2O)(CN)_4]^{2-}$ complex and the pyridine-2-carboxylate ligand was determined by means of spectrophotometry at 350 nm by a least-squares fit of the absorbance *vs.* concentration data shown in Figure 7.2 to eq. 7.9.

$$\mathbf{A_{obs} = \frac{A_M + A_{ML} K'[O=N]}{1 + K'[O=N]}} \qquad \mathbf{7.9}$$

As mentioned earlier, eq. 7.9 is derived from Beer's law, the mass balance equation and the definition of K′ for the overall reaction of the $[MnN(H_2O)(CN)_4]^{2-}$ with the different pyridine carboxylate ligands (O-N) (see Appendix B.2). In eq. 7.9 A_M and A_{ML} represent the absorbance of the $[MnN(H_2O)(CN)_4]^{2-}$ and $[MnN(\eta^2\text{-O=N})(CN)]^{2-}$ complexes, A_{obs} the observed absorbance and [O=N] the concentration of the different pyridine carboxylate ligands. The four bidentate pyridine carboxylate ligands used during this study were pyridine-2-carboxylate, pyridine-2,3-carboxylate, pyridine-2,4-carboxylate and pyridine-2,5-carboxylate anions. However, no reaction was observed between the $[MnN(H_2O)(CN)_4]^{2-}$ complex and pyridine-2,6-carboxylate anions and it is thought that it might be due to steric interaction between the nitrido ligand in the axial position and the second carboxylate group in the 6th position of the aromatic ring.

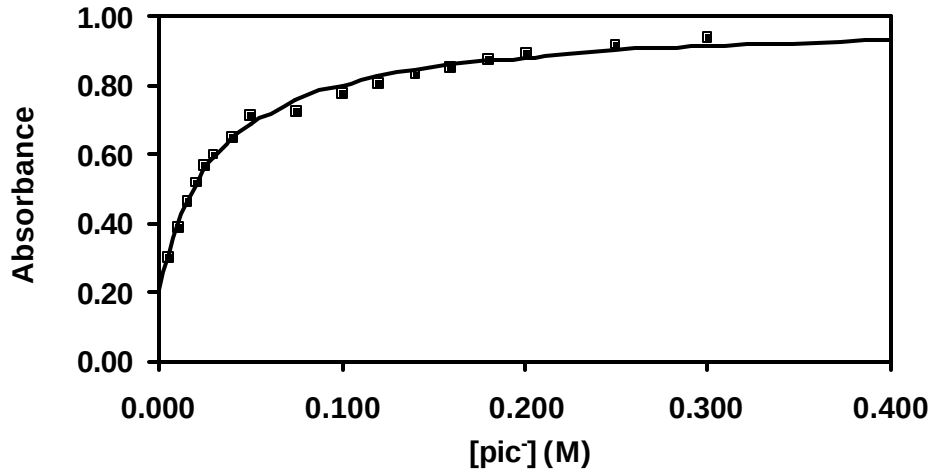

Figure 7.2: Absorbance *vs.* [pic⁻] at 25.6 °C, $[Mn]_T = 5.26 \times 10^{-4}$ M, μ = 1.0 M (KNO_3), pH = 10.0, ? = 350.0 nm.

A careful analysis of the absorbance *vs.* time data at 350 nm in this study revealed that only one reaction is observed at this wavelength. Figure 7.3 shows the temperature and concentration dependence of the pseudo first-order rate constant (k_{obs}) for the second slow reaction at 350 nm. The k_{obs} *vs.* [pic^-] data in Figure 7.3 was fitted to eq. 7.6 and the values of k'_1 ($k'_1 = k_2K_1$) and k'_{-1} are given in Table 7.2. The term k'_{-1} represents the contribution of the reverse reaction or the recoordination of the cyanide anion. However, the influence of this rate constant (k'_{-1}) could not be determined due the fact that only a very small excess of added cyanide anions severely retarded the rate of the reaction between $[MnN(H_2O)(CN)_4]^{2-}$ and pic^-. This situation is thus complicated due to the fact that addition of excess free CN^- leads to the formation of the $[MnN(CN)_5]^{3-}$ due to the reverse reaction in the initial equilibrium for the formation of the $[MnN(H_2O)(CN)_4]^{2-}$ complex from $[MnN(CN)_5]^{3-}$ (see reaction **A**, Scheme 7.2).

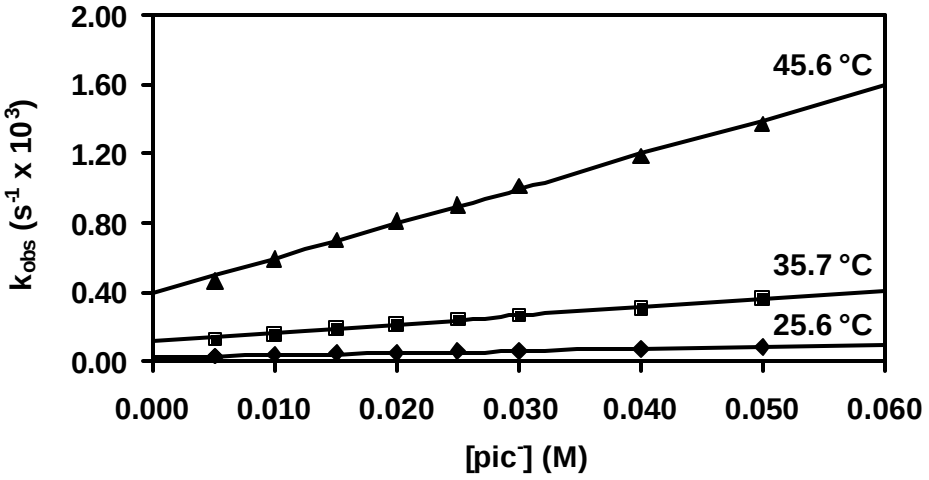

Figure 7.3: Temperature and [pic⁻] dependence of the pseudo first-order rate constant (k_{obs}) for the second reaction between $[MnN(H_2O)(CN)_4]^{2-}$ and pic^- anions, $[Mn]_T = 5.26 \times 10^{-4}$ M, μ = 1.0 M (KNO_3), pH = 10.0, ? = 350 nm.

The pH dependence of the pseudo first-order rate constant for the second reaction is illustrated in Figure 7.4. The values of the different rate constants and the acid dissociation constant were obtained from a least-squares fit of the data in Figure 7.4 to eq. 7.7 and are reported in Table 7.2. The reactions could not be studied at pH values higher than 14 due to a rapid decomposition of the complexes at very high concentrations of OH^-. Thus, the solid line in Figure 7.4 is a simulated fit of the pH s-curve, using the obtainable data points, to eq. 7.7. It is however interesting to note that the observed rate constant increases at higher pH values, similar to that observed for the reaction of $[MoO(H_2O)(CN)_4]^{2-}$ with 1,10-phenanthroline.[15] However, the tungsten(IV) system[17] showed a decrease in k_{obs} at higher pH-values.

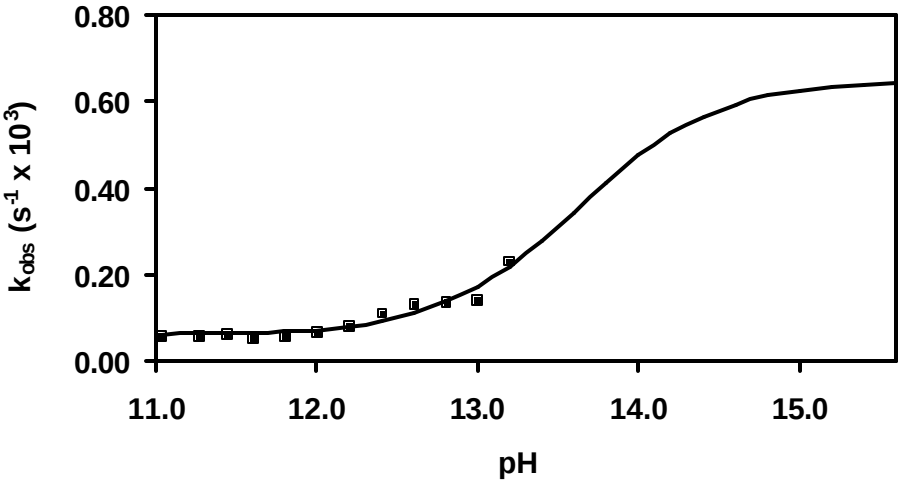

Figure 7.4: pH dependence of the pseudo first-order rate constant for the second reaction between $[MnN(H_2O)(CN)_4]^{2-}$ and pic^- anions at 25.3 °C, $[M]_T = 5.26 \times 10^{-4}$ M, $[pic^-] = 0.020$ M, μ = 1.0 M (KNO_3), ? = 350 nm.

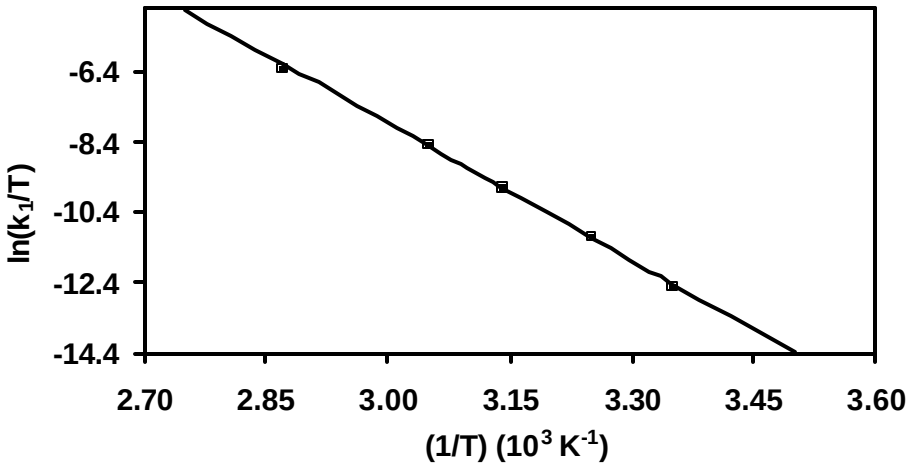

Figure 7.5: Plot of $\ln k_1/T$ *vs.* 1/T for the second reaction between $[MnN(H_2O)(CN)_4]^{2-}$ and pic^- anions.

The activation parameters of the overall reaction between the $[MnN(H_2O)(CN)_4]^{2-}$ complex and pic^- anions were determined by a least-squares fit of the temperature dependency data of the pseudo first-order rate constant (k'_1, see Figure 7.5) to the Eyring equation (eq. 7.8).

7.4.3. Reaction with pyridine-2,3-dicarboxylate (2,3-dipic^{2-})

The UV/visible spectrum of the reaction between $[MnN(H_2O)(CN)_4]^{2-}$ and pyridine-2,3-dicarboxylate (2,3-dipic^{2-}) anions showed only one maximum at 356 nm. The stability constant of the $[MnN(2,3\text{-dipic})(CN)_4]^{3-}$ or equilibrium constant (K′, see Table 7.2) of the overall reaction was determined by means of spectrophotometry by a least-squares fit of the absorbance *vs.* [2,3-dipic^{2-}] data in Figure 7.6 to eq. 7.9.

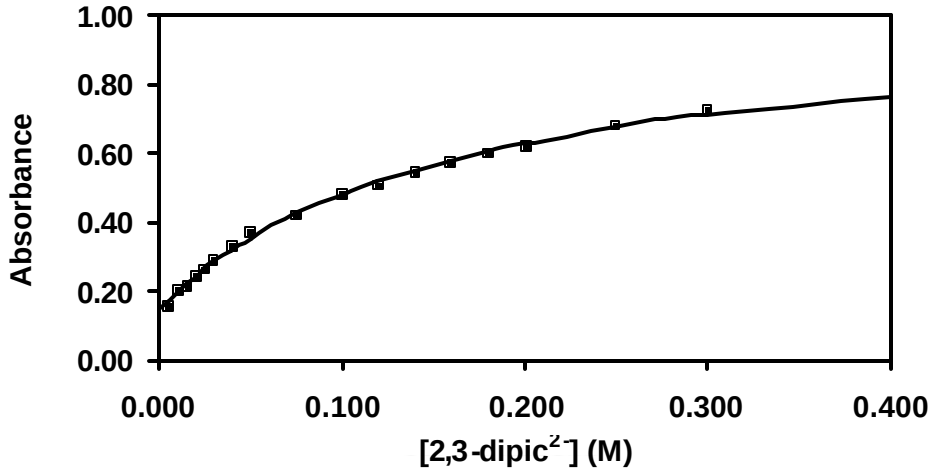

Figure 7.6: Absorbance *vs.* [2,3-dipic^{2-}] at 25.4 °C, μ = 1.0 M (KNO_3), [Mn] = 5.26 x 10^{-4} M, ? = 365.0 nm, pH = 10.0.

The plots of the absorbance *vs.* time data for the reaction of the $[MnN(H_2O)(CN)_4]^{2-}$ complex with different concentrations of 2,3-dipic^{2-} anions showed only one distinct reaction. Figure 7.7 shows the temperature and [2,3-dipic^{2-}] dependence of the pseudo first-order rate constant for the second slow reaction between $[MnN(H_2O)(CN)_4]^{2-}$ and 2,3-dipic^{2-} anions. The k_{obs} *vs.* [pic$^-$] data in Figure 7.7 was fitted to eq. 7.6 and the values of k'_1 ($k'_1 = k_2K_1$) and k'_{-1} are given in Table 7.2.

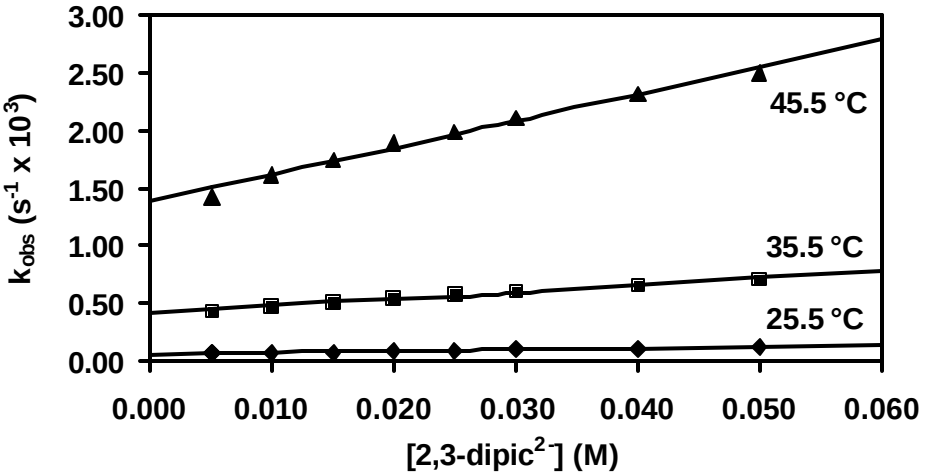

Figure 7.7: Temperature and [2,3-dipic^{2-}] dependence of the pseudo first-order rate constant (k_{obs}) for the second slow reaction, $[Mn]_T$ = 5.26 x 10^{-4} M, μ = 1.0 M (KNO_3), pH = 10.0, ? = 365 nm.

The pH dependence of the overall reaction between $[MnN(H_2O)(CN)_4]^{2-}$ and 2,3-dipic^{2-} anions is shown in Figure 7.8. The k_{obs} *vs.* pH data in Figure 7.8 was fitted to eq. 7.7 and the values for different rate constants obtained are given in Table 7.2. The solid line in Figure 7.7 represents a least-squares fit of the few obtainable data points to eq. 7.7. It is however unfortunate that only a few data points were obtained due to the fact that the complexes decomposed at higher $[OH^-]$. The UV/visible spectra taken overnight of the $[MnN(OH)(CN)_4]^{3-}$ complex in a 1M NaOH solution (pH = 14) showed that this complex is relatively stable at this high $[OH^-]$.

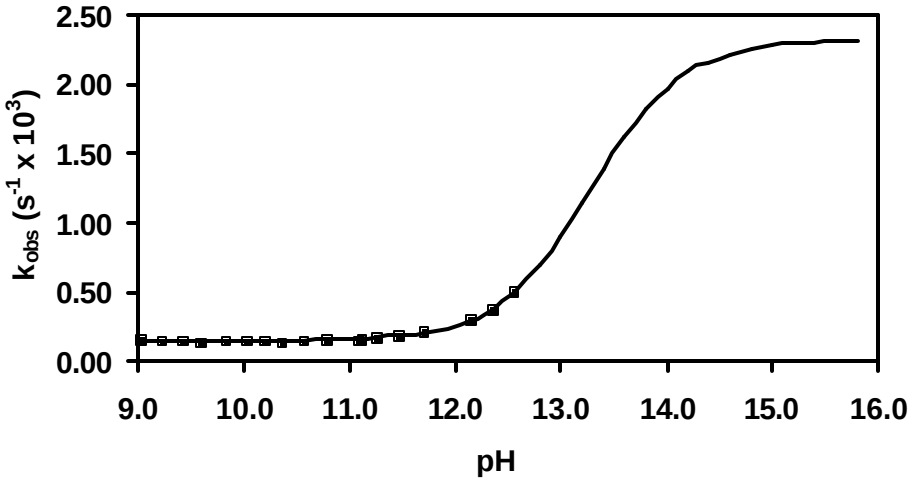

Figure 7.8: pH dependence of the pseudo first-order rate constant for the slow reaction between $[MnN(H_2O)(CN)_4]^{2-}$ and 2,3-dipic^{2-} anions at 25.4 °C, $[M]_T$ = 5.26 x 10^{-4} M, [2,3-pic$^-$] = 0.020 M, μ = 1.0 M (KNO_3), ? = 365 nm.

However, as mentioned above, any attempt to determine the k'_2 and k'_{-2} rate constants at pH 14 failed due to the rapid decomposition of the complexes at these high concentrations of OH^-.

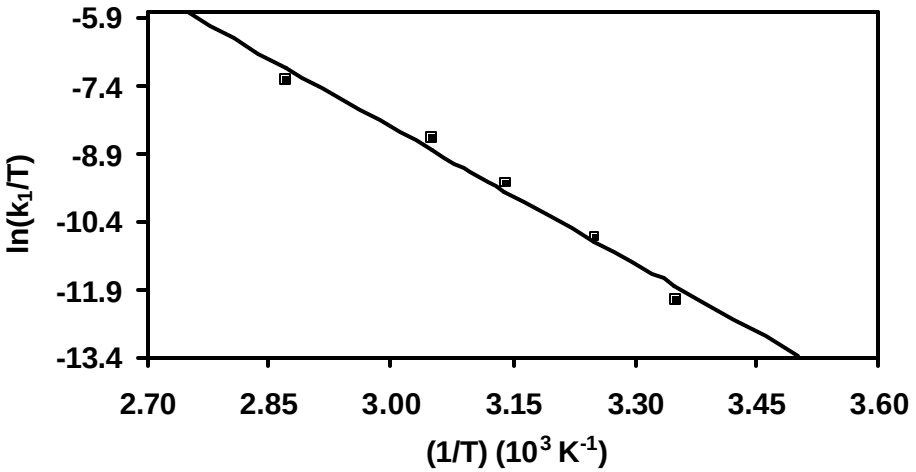

Figure 7.9: Plot of lnk_1/T *vs.* 1/T for the second slow reaction between $[MnN(H_2O)(CN)_4]^{2-}$ and 2,3-dipic^{2-} anions.

The activation parameters of the overall reaction between the $[MnN(H_2O)(CN)_4]^{2-}$ complex and 2,3-dipic^{2-} anions were determined by a least-squares fit of the temperature dependency data of the pseudo first-order rate constant (k'_1, see Figure 7.9) to the Eyring equation (eq. 7.8).

7.4.4. Reaction with pyridine-2,4-dicarboxylate (2,4-dipic^{2-})

The stability constant (K′, Table 7.2) for the overall reaction between the $[MnN(H_2O)(CN)_4]^{2-}$ complex and pyiridine-2,4-dicarboxylate anions (2,4-dipic^{2-}) was determined by means of spectrophotometry from a least-squares fit of the absorbance *vs.* [2,4-dipic^{-}] data to eq. 7.9 in Figure 7.10. Only one absorbance maximum at 373 nm was detected in the UV/visible spectrum of the reaction between the mentioned anions and a plot of the absorbance *vs.* time data showed only one distinct slow reaction at 375 nm.

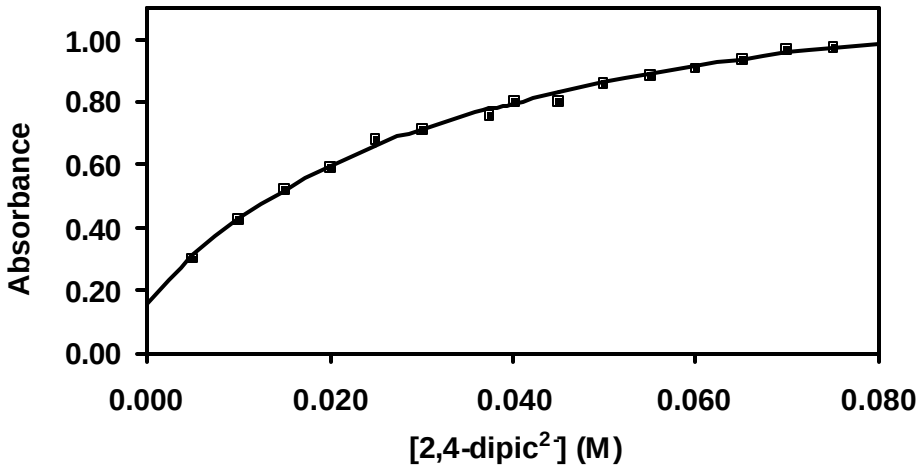

Figure 7.10: Absorbance *vs.* [2,4-dipic^{2-}] at 25.3 °C, [Mn] = 5.26 x 10^{-4} M, μ = 1.0 M (KNO_3), pH = 10.0, ? = 375.0 nm.

The [2,4-dipic^{2-}] and temperature dependencies of the pseudo first-order rate constant for the second reaction between the $[MnN(H_2O)(CN)_4]^{2-}$ and 2,4-dipic^{2-} anions are presented in Figure 7.11. The overall rate constants k'_1 and k'_{-1} were obtained from a least-squares fit of the data to eq. 7.6 in Figure 7.11 and the values

of k'_1 and k'_{-1} are obtained from the slopes and the intercepts of these plots respectively (see Table 7.2).

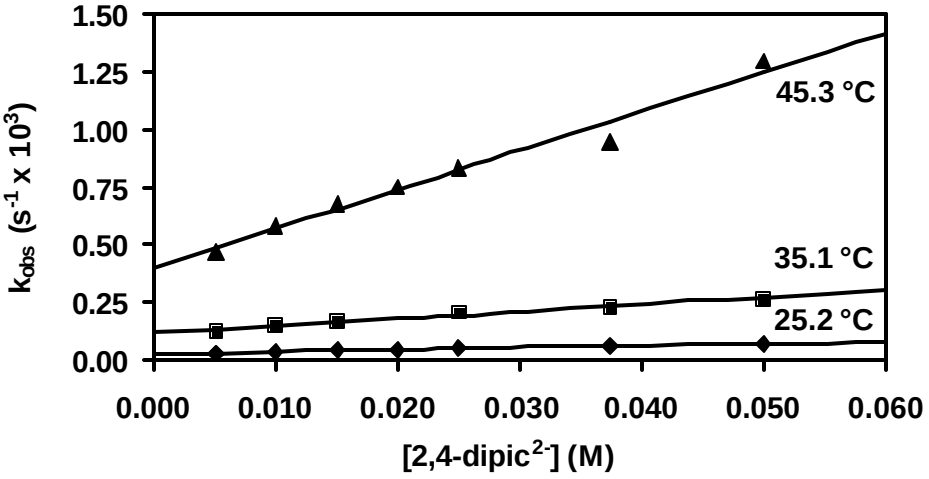

Figure 7.11: Temperature and [2,4-dipic^{2-}] dependence of the pseudo first-order rate constant (k_{obs}) for the second slow reaction, $[Mn]_T$ = 5.26 x 10^{-4} M, μ = 1.0 M (KNO_3), pH = 10.0, ? = 375 nm.

Since it was very difficult to obtain any good quality data for the determination of the rate constants of reaction between $[MnN(H_2O)(CN)_4]^{2-}$ and 2,4-dipic^{2-} at higher pH values, the pH- and [2,4-dipic^{2-}] dependencies at high pH of the pseudo first-order rate constant were not determined for these reactions.

The temperature dependency of the pseudo first-order rate constant (k'_1, see Figure 7.12) of the second step in the reaction between $[MnN(H_2O)(CN)_4]^{2-}$ and 2,4-dipic^{2-} was used to obtain the activation parameters of the overall process and the values for $\Delta H^?$ and $\Delta S^?$ are given in Table 7.2.

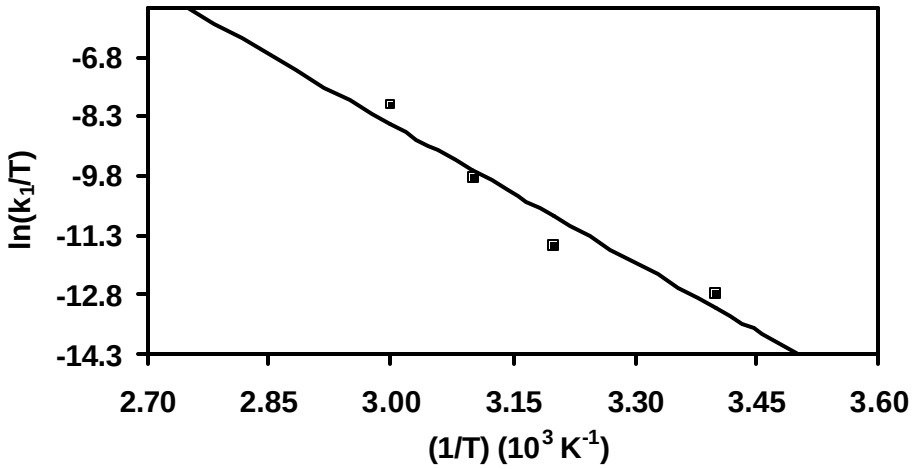

Figure 7.12: Plot of $\ln k_1/T$ *vs.* 1/T for the second slow reaction between $[MnN(H_2O)(CN)_4]^{2-}$ and 2,4-dipic^{2-} anions.

7.4.5. Reaction with pyridine-2,5-dicarboxylate (2,5-dipic^{2-})

The UV/visible spectra of the reaction between the $[MnN(H_2O)(CN)_4]^{2-}$ complex and pyridine-2,5-dicarboxylate (2,5-dipic^{2-}) showed only one maximum at 366 nm and examination of the absorbance *vs.* time data showed the presence of only one reaction at this wavelength. The stability constant (K') of the $[MnN(2,5\text{-dipic})(CN)_4]^{2-}$ complex was determined by a least-squares fit of the absorbance *vs.* [2,5-dipic^{2-}] data in Figure 7.13 to eq. 7.9 (see Table 7.2).

The plots in Figure 7.14 show the [2,5-dipic^{2-}] dependency of the pseudo first-order rate constant at three different temperatures. The k'_1 and k'_{-1}-values were obtained from a least-squares fit of the data in Figure 7.14 to eq. 7.6 and these values are given in Table 7.2. As mentioned earlier, the term k'_1 represents the product of the equilibrium constant (K_1) for the first step and the forward rate constant (k_2) for the second step in eq. 7.6. The term k'_{-1} (k'_{-2} from eq. 7.5) represents the reverse reaction for the second step of the uptake of cyanide anions.

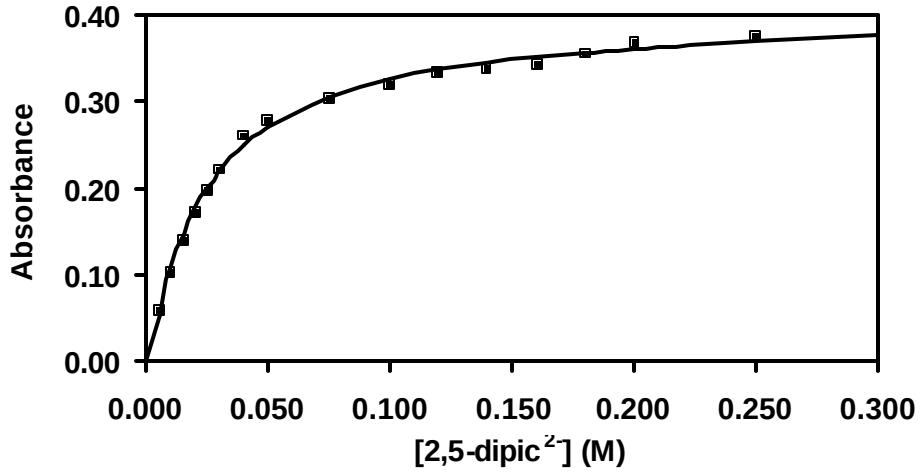

Figure 7.13: Absorbance *vs.* [2,5-dipic^{2-}] at 25.6 °C, μ = 1.0 M (KNO_3), [Mn] = 5.26 x 10^{-4} M, ? = 385.0 nm, pH = 10.0.

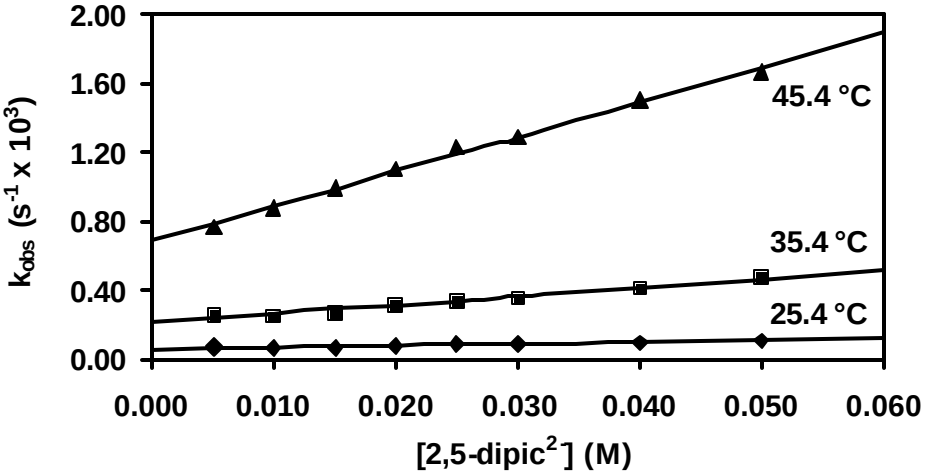

Figure 7.14: Temperature and [2,5-dipic^{2-}] dependence of the pseudo first-order rate constant (k_{obs}) for the second slow reaction, $[Mn]_T$ = 5.26 x 10^{-4} M, μ = 1.0 M (KNO_3), pH = 10.0, ? = 385 nm.

Due to the decomposition of the product of the reaction between $[MnN(H_2O)(CN)_4]^{2-}$ and 2,5-dipic^{2-} at high [OH^-], the pH- and [2,5-dipic^{2-}] dependencies of the pseudo first-order rate constant of the reaction with this bidentate ligand were not determined.

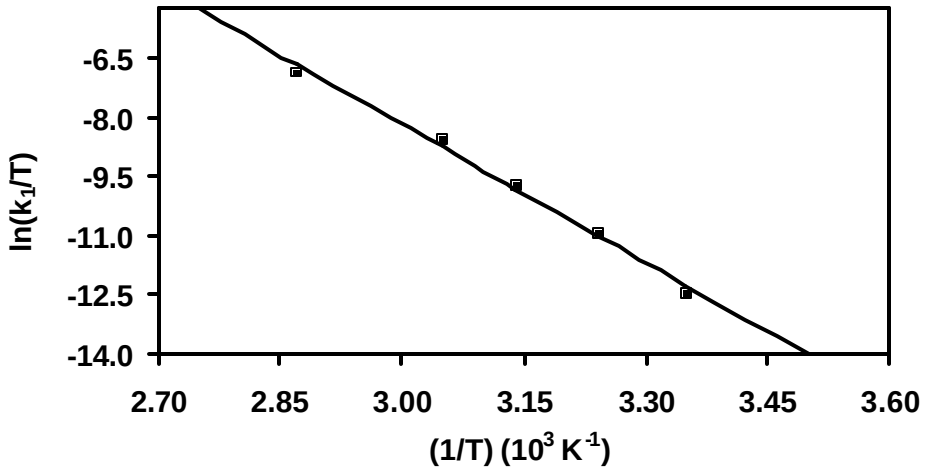

Figure 7.15: Plot of $\ln k_1/T$ *vs.* 1/T for the second slow reaction between $[MnN(H_2O)(CN)_4]^{2-}$ and 2,5-dipic^{2-} anions.

The activation parameters ($\Delta H^{?}$ and $\Delta S^{?}$) of the overall reaction between $[MnN(H_2O)(CN)_4]^{2-}$ and 2,5-dipic^{-} were obtained from a least-squares fit of the Eyring equation (eq. 7.8) to the k'_1 values *vs.* the different temperatures (see Figure 7.15). The $\Delta H^{?}$ and $\Delta S^{?}$ values for the overall reaction between $[MnN(H_2O)(CN)_4]^{2-}$ and 2,5-dipic^{-} are given in Table 7.2.

Table 7.2: Kinetic data for the reactions between the different picolinate type ligands and $[MnN(H_2O)(CN)_4]^{2-}$, see also Scheme 7.2.

Constant	pic$^-$	2,3-dipic^{2-}	2,4-dipic^{2-}	2,5-dipic^{2-}
25 °C				
K' [a]	33(4)	6.4(6)	30(4)	43(4)
k'_1 ($M^{-1}s^{-1}$) [b]	1.15(4) x 10^{-3}	1.1(1) x 10^{-3}	8.5(5) x 10^{-4}	1.08(4) x 10^{-3}
k'_{-1} (s^{-1}) [c]	3.1(1) x 10^{-5}	7.2(2) x10^{-5}	3.2(1) x 10^{-5}	5.5(1) x 10^{-5}
K'_1 (M^{-1}) [d]	37.1(1)	15.3(1)	26.6(1)	19.6(1)
pK_{a1} [e]	13.6(6)	13.3(2)	-	-
k'_1 ($M^{-1}s^{-1}$) [e]	2.0(2) x 10^{-3}	7.4(1) x 10^{-3}	-	-
k'_{-1} (s^{-1}) [e]	1.7(5) x 10^{-7}	1(2) x 10^{-6}	-	-
k'_2 ($M^{-1}s^{-1}$) [e]	0.02(2)	0.12(4)	-	-
k'_{-2} (s^{-1}) [e]	6(9) x 10^{-5}	2(2) x 10^{-4}	-	-
35 °C				
k'_1 ($M^{-1}s^{-1}$) [b]	5.0(1) x 10^{-3}	6.1(2) x 10^{-3}	3.1(2) x 10^{-3}	5.6(1) x 10^{-3}
k'_{-1} (s^{-1}) [c]	1.16(1) x 10^{-4}	4.2(1) x 10^{-4}	1.2(1) x 10^{-4}	1.94(4) 10^{-4}
K'_1 (M^{-1}) [d]	43.1(2)	14.5(1)	25.8(1)	28.9(1)
45 °C				
k'_1 ($M^{-1}s^{-1}$) [b]	0.0199(5)	0.023(1)	0.017(1)	0.0201(6)
k'_{-1} (s^{-1}) [c]	4.0(1) x 10^{-4}	1.39(3) x 10^{-3}	4.0(3) x 10^{-3}	6.9(2) x 10^{-4}
K'_1 ($^{M-1}$) [d]	49.8(3)	16.5(1)	4.3(1)	29.1(1)
$\Delta H^?$ ($kJmol^{-1}$) [f]	104(2)	80(2)	105(3)	94.6(7)
$\Delta S^?$ ($JK^{-1}mol^{-1}$) [f]	48.7(5)	-25(5)	49(10)	20(2)

[a] From data in Figure 7.2, Figure 7.6, Figure 7.10, Figure 7.13 and eq. 7.9.

[b] Slopes of Figure 7.3, Figure 7.7, Figure 7.11, Figure 7.14, and eq. 7.6.

[c] Y-intercepts of Figure 7.3, Figure 7.7, Figure 7.11, Figure 7.14, and eq. 7.6.

[d] $K'_1 = k'_1/k'_{-1}$

[e] Data in Figure 7.4, Figure 7.8 and eq. 7.7.

[f] Eq. 7.8

7.5. Discussion

7.5.1. Reactions of $[MnN(H_2O)(CN)_4]^{2-}$ with monodentate ligands

Results from previous kinetic studies of the reactions of $[MN(H_2O)(CN)_4]^{n-}$ [M = rhenium(V) and osmium(VI)] with monodentate ligands have shown that only the aqua ligand is substituted in these complexes.[1,2] These studies have also shown that the hydroxo complex is formed upon deprotonation of the aqua complex and that the hydroxo complex is inert towards monodentate substitution reactions. A dissociative mechanism for the substitution of the aqua ligand in $[MN(H_2O)(CN)_4]^{n-}$ by monodentate nucleophiles was proposed. However, in the $[MO(OH)(CN)_4]^{n-}$ complexes, OH^- exchange gave some evidence suggesting an associative mechanism for the OH^- exchange in these complexes.[18]

The syntheses of the nitridotetracyano complexes of rhenium(V) and osmium(VI) usually produced the aqua complexes as starting compounds for the syntheses of the different monodentate substituted complexes and as one of the reactants during kinetic investigations.[1,2] However, $[(CH_3)_4N]_2Na[MnN(CN)_5]\cdot H_2O$ (see § 3.3.3) is obtained as the starting compound for the synthesis of the different nitridocyano complexes of manganese(V) and as one of the reactants in the kinetic studies with mono- and bidentate ligands (see § 7.3 and 7.4). As mentioned earlier, the $[MnN(CN)_5]^{3-}$ anion dissociates in an aqueous solution (even at high $[CN^-]$, ~ 0,3 M) with the dissociation of the *trans*-bonded cyano ligand. The crystal structure of $(Ph_4P)_2[MnN(CN)_4]\cdot 2H_2O$ (see § 4.4), for example, determined from crystals obtained after addition of Ph_4PCl or Ph_4AsCl to a CN^--solution (~ 0.3 M) of the $[MnN(CN)_5]^{3-}$ complex showed that the sixth coordination site *trans* to nitrido ligand is vacant.[30] Thus, crystals of the monodentate substituted $[MnN(L)(CN)_4]^{n-}$ complexes (L = monodentate ligand) could only be crystallized from solutions with very high concentrations (~ 1 M) of the monodentate ligand (see § 3.3.6 to 3.3.10). However, the concentration of the aqua ligand in solution is *ca.* 55 M and it is presumed that the $[MnN(H_2O)(CN)_4]^{2-}$ anion exists in solution after the dissociation of the *trans*-

[30] Bendix, J.; Meyer, K.; Weyhermüller, T.; Bill, E.; Metzler-Nolte, N.; Wieghardt, K., *Inorg.Chem.*, **1998**, *37*, 1767.

bonded ligand (CN^-) or that the aqua ligand is at least in the very near vicinity of the sixth coordination site. Unfortunately, the crystal structure of the $[MnN(H_2O)(CN)_4]^{2-}$ complex has not been determined to date and thus, the crucial question of whether the aqua ligand is bonded *trans* to the nitrido ligand or not remains unanswered for the moment. It was decided to use the $[MnN(H_2O)(CN)_4]^{2-}$ formula for the $[MnN(CN)_4]^{2-}$/$[MnN(H_2O)(CN)_4]^{2-}$ species as a standard in the discussion of the results obtained from the kinetic studies. The dissociation of the $[MnN(CN)_5]^{3-}$ complex to form the aqua species (see reaction **A**, Scheme 7.2) was ignored during the course of this kinetic investigation. The concentration of $[MnN(H_2O)(CN)_4]^{2-}$ can also be estimated, assuming the $[CN^-]_{free}$ is at $[Mn]_T = 5 \times 10^{-4}$ M, thus, more than 99% of $[Mn(CN)_5]^{3-}$ will dissociate to form the $[MnN(H_2O)(CN)_4]^{2-}$ complex in solution*.

As mentioned earlier (§ 7.3), the monodentate substitution reactions of the aqua ligand in $[MnN(H_2O)(CN)_4]^{2-}$ are very fast and the pseudo first-order rate constants could not be obtained from absorbance *vs.* time data for these reactions. In fact, the absorbance *vs.* time data obtained using a 3rd generation stopped-flow spectrophotometer, a machine that is specifically designed for determining the rates of these fast reactions, only showed the mixing of the two solutions as well as a higher absorbance maximum for each higher concentration of CN^- anions, for example. The equilibrium constant (K_1 = 168(20) M^{-1}) for the reaction between $[MnN(H_2O)(CN)_4]^{2-}$ and CN^- (see reaction **A**, Scheme 7.1) was determined from the absorbance *vs.* $[CN^-]$ data (Figure 7.1).

Results from the kinetic studies of the reactions between the $[MX(H_2O)(CN)_4]^{n-}$ complexes (M = molybdenum(IV), tungsten(IV), technetium(V), rhenium(V) and osmium(VI), X = nitrido or oxo) and different monodentate ligands are shown in Table 7.3. The results show that there is an increase in the reaction rate (k_1) of by a factor of 50-200 for the group 6 elements and for the group 7 elements, an increase by a

---

* $[MnN(CN)_5]^{3-} \rightleftharpoons^{K} [MnN(H_2O)(CN)]^{2-} + CN^-$

$K_e = \dfrac{[MnN(H_2O)(CN)_4^{2-}][CN^-]}{[MnN(CN)_5^{3-}]}$

\ $[MnN(CN)_5^{3-}] = 1.5 \times 10^{-9}$ M (see Appendix B.5)

factor of ~ 6300 upon going from the second- to the third-row elements. This suggests that the metal-aqua bond is stronger in the third-row elements than in the second-row elements, as is expected. On going to the first-row elements, these metal-aqua bonds should be even weaker compared to the second- and third-row elements, which means that the aqua substitution reactions should also be much faster. The rate of the reaction between $[ReN(H_2O)(CN)_4]^{2-}$ and CN^- in Table 7.3 was determined on a stopped-flow spectrophotometer and with the above-mentioned in mind, the rate of the reaction between $[MnN(H_2O)(CN)_4]^{2-}$ and CN^- should be too fast to determine with a stopped-flow spectrophotometer. The results also indicate that the rate of the reverse reaction (k_{-1}) or the dissociation of the CN^- ligand has a significant contribution in the overall process. The very large difference found for the values of k_1 for the complexes of the second and third-row and possibly the first-row elements may also point towards a dissociative mechanism for the substitution reactions. A weaker metal-aqua bond for the second and possibly the first-row elements is also evident from the higher pK_a values for the second and third row complexes. A weaker metal-oxygen bond will strengthen the oxygen-hydrogen bonds in the aqua ligand with a resulting higher pK_a value.

Another significant and interesting feature about the results in Table 7.3 is the decrease in reaction rate upon going from group 6 to group 7 elements. The metal ions in group 6 have a formal charge of +4 and those of group 7 a formal charge of +5 in the $[MX(H_2O)(CN)_4]^{n-}$ complexes. The reaction rates of the $[MoO(H_2O)(CN)_4]^{2-}$ complex are about 10 times faster than the $[TcO(H_2O)(CN)_4]^-$ complex and the rates for $[WO(H_2O)(CN)_4]^{2-}$ about 820 times faster than for $[ReO(H_2O)(CN)_4]^-$. This indicates that the aqua ligand is more strongly bonded to the metal ion with the higher formal charge, probably due to a stronger dipole-ion interaction between the aqua ligand and the metal ion with the higher charge. This stronger metal-aqua bond is also evidenced by the very large decrease in the pK_a values of the aqua complexes upon going from a metal with a +4 formal charge to one with a +5 formal charge. The mentioned decrease in reaction rate with an increase in the formal charge of the metal ion also suggests a dissociative mechanism since ease of bond breaking is apparently very significant in the determination of the relative reactivity of these complexes.

Table 7.3: Kinetic data for the reaction of $[MX(H_2O)(CN)_4]^{n-}$ complexes with different monodentate ligands (L) at 25 °C.

Metal	X	L	pK_{a1}	k_1 (M^{-1} s^{-1})	K_1 (M^{-1})	$\Delta S^{\neq}$ (JK^{-1} mol^{-1})	Ref.
Mo^{IV}	O	CN^- [a]	10.0	116(2)	95(5)	-53(14)	3,9
	O	F^- [b]		18.7(6)	12.1(9)	-59(13)	8
W^{IV}	O	CN^-	7.8	1.15(3)	1.1(1) X 10^3	12(20)	4,10
	O	NCS^-		2.9(1)	2.0(1)	8(9)	12
	O	F^- [a]		1.06(3) x 10^{-3}	1.4(2) x 10^2	-28(10)	31
	O	N_3^- [c]		4.2(1)	4.8(11)	-10(8)	11
	O	py		6.9(4)	0.5(1)	101(6)	12
Tc^{V}	O	NCS^-	2.9	22.2(3)	54(2)	-9(12)	5
Re^{V}	O	NCS^-	1.4	3.48(4) x 10^{-3}	87(7)	-46(20)	13
Mn^{V}	N	CN^-	~ 13	> 20000	168(20)	-	d
Re^{V}	N	CN^- [b]	11.7	7.2(4) x 10^3	600(100)	-40(6)	1
Os^{VI}	N	N_3^-	7.43	1.89(7)	189(8)	-45(3)	2

[a] at 20 °C [b] at 15 °C

[c] $\Delta V^{\neq}$ = 10.6(5) cm^3 mol^{-1} [d] This work

Upon comparing the values of the k_1 in Table 7.3 for the reactions of the oxo and nitrido complexes of rhenium(V) an even more spectacular effect of bond strength on the relative reactivity of these complexes is observed. The nitrido complex with the weak metal-aqua bond [Re-OH_2 = 2.496(7) Å][32] reacts about 10^6 times faster than the oxo with the much stronger metal-aqua bond [Re-OH_2 = 2.142(7) Å].[33] The comparison of the rate constants given in Table 7.3 is not made with the same entering nucleophiles, since it was not possible to study the reaction of the oxo complex with cyanide ions (the $[ReO(H_2O)(CN)_4]^-$ complex exists only at a low pH value) and the reaction of $[ReN(H_2O)(CN)_4]^{2-}$ with NCS^- is too fast at the high $[NCS^-]$ that is necessary as a result of the relative low stability constant of the $[ReN(NCS)(CN)_4]^{3-}$ complex. However, it is reasonable to assume that the rate constants of these complexes with CN^- should be about the same as those with NCS^-

[31] Leipoldt, J.G.; Basson, S.S.; Roodt, A.; Potgieter, I.M., *S. Afr. J. Chem.*, **1986**, *39*, 179.
[32] Purcell W.; Potgieter I. M.; Damoense L. J.; Leipoldt J. G., *Transition Met. Chem.*, **1992**, *17*, 387.
[33] Purcell, W.; Roodt, A.; Basson, S.S.; Leipoldt, J.G., *Transition Met. Chem.*, **1990**, *15*, 239.

since it was shown that the substitution reactions of these types of complexes proceed *via* a dissociative mechanism. Thus, the effect of the entering ligand will be relatively small. The effect of the rhenium-aqua bond strengths in the oxo and nitrido complexes is also evidenced by the very large increase in the pK_a value of 1.4 for the oxo complex to about 12 for the nitrido complex. This very high pK_a value for the nitrido complex points to a very weakly bonded aqua ligand and this is in agreement with the two above-mentioned rhenium-aqua bond distances found in the crystal structure determinations of the oxo and nitrido complexes. The large dependency of the rate of substitution on the rhenium-aqua distance, as well as the high reactivity of the nitrido complex also suggests a dissociative mechanism.

Thus, with all the above-mentioned in mind, it is expected that the $[MnN(H_2O)(CN)_4]^{2-}$ complex will have a higher pK_a value compared to the $[ReN(H_2O)(CN)_4]^{2-}$ complex, due to the fact that upon going from the third to the second row and then the first row elements the metal-aqua bond is expected to weaken significantly as seen from the above-mentioned results. The $[MnN(H_2O)(CN)_4]^{2-}$ complex should also have a much higher reactivity compared to the $[ReN(H_2O)(CN)]^{2-}$ complex and the substitution reactions of the aqua ligand in $MnN(H_2O)(CN)_4]^{2-}$ should also proceed *via* a dissociative mechanism.

7.5.2. Reactions of $[MnN(H_2O)(CN)_4]^{2-}$ with bidentate ligands

Results from the kinetic studies of the substitution reactions between the $[MoO(H_2O)(CN)_4]^{2-}$ complex and the bidentate ligands 1,10-phenanthroline and 2,2′-bipyridine suggested that the aqua substitution is the rate determining step, which is followed by a fast ring-closure as the second step (see Table 7.4).[15,16] The results obtained for the bidentate substitution reactions of the $[MoO(H_2O)(CN)_4]^{2-}$ complex in these studies were consequently interpreted in terms of eq. 7.2, the same way as for the monodentate substitution and the pH and ligand dependence could be explained satisfactorily using this equation.

Table 7.4: Kinetic data for the reaction of $[MX(H_2O)(CN)_4]^{n-}$ complexes with different bidentate ligands (LL) at 25 °C.

M	X	LL	pK_{a1}	k_1 ($M^{-1}s^{-1}$)	K_1 (M^{-1})	k_2 ($M^{-1}s^{-1}$)	K_2 (M^{-1})	K' [a] (M^{-1})	Ref.
Mo^{IV}	O	phen	10.24(7)	$2.68(2) \times 10^{-1}$	558(20)	1.04(4)		560(30)	15
	O	bipy		0.26(1)	$3.8(3) \times 10^{2}$	-	-	1.1(1)	16
W^{IV}	O	pic^-	7.4(2)	0.80(8)	1.1(2)	$1.70(8) \times 10^{-3}$	10(2)	13(2)	17
Mn^{V}	N	pic^-	13.6(6)	$1.15(4) \times 10^{-3}$ [c]	37 [d]			33(4)	e
		$2,3\text{-dip}^{2-}$ [b]	13.3(2)	$1.1(1) \times 10^{-3}$ [c]	15 [d]			6.4(6)	e
		$2,4\text{-dip}^{2-}$ [b]		$8.5(5) \times 10^{-4}$ [c]	27 [d]			30(4)	e
		$2,5\text{-dip}^{2-}$ [b]		$1.08(4) \times 10^{-3}$ [c]	20 [d]			43(4)	e

[a] K' = overall equilibrium constant

[b] $2,3\text{-dip}^{2-}$ = 2,3-dipic^{2-} for example

[c] $k_1 = k'_1$ ($k'_1 = K_1k_2$) (see Table 7.2)

[d] $K_1 = K'_1$ ($K'_1 = k'_1/k'_{-1}$) (see Table 7.2)

[e] This work

Scheme 7.2 is based on the results obtained from the crystal structure determination of the $(Ph_4As)_2[WO(\eta^2\text{-pic})(CN)_3]\cdot 3H_2O$ complex[21] and the kinetic study of the bidentate substitution reaction of $[WO(H_2O)(CN)_4]^{2-}$ with pic^- anions.[17] The same results were also obtained from the crystal structures of $(Ph_4As)_2[MnN(\eta^2\text{-pic})(CN)_3]\cdot 4H_2O$, $(Ph_4As)_2[MnN(\eta^2\text{-quin})(CN)_3]\cdot 3H_2O$ and $(Ph_4As)_2[MoO(\eta^2\text{-pic})(CN)_4]\cdot 3H_2O$ (see § 6.3, 6.4 and 6.5). In all these structure determinations the isomers obtained contained the carboxylate moiety *trans* to the nitrido or oxo ligand, which showed that aqua ligand was substituted during the first step, since it is known that the carboxylate group in pyridine-2-carboxylate will coordinate before the pyridine nitrogen atom. Furthermore, the coordination of the entering monodentate ligand to the metal center, as manifested in the stability of the $[MX(L)(CN)_4]^{n-}$ complex formed, is very much dependent on the coordination capability of the particular ligand. The stability constants for the $[WO(L)(CN)_4]^{m-}$ complexes (L = CN^-, F^-, N_3^-, NCS^- anions and py) were determined as 1.1(1) x 10^3, 1.4(2) x 10^2, 4.8(11), 2.0(1), 0.5(1) M^{-1} during previous kinetic studies[10,11,12,31] of the monodentate substitution of the aqua ligand in the $[WO(H_2O)(CN)_4]^{2-}$ complex. The value of 1.0(2) M^{-1} determined for the first step in the study of the reaction between $[WO(H_2O)(CN)_4]^{2-}$ and pic^- is in direct agreement with the above mentioned stability constants since the carboxylate group is a weak σ donor. Only very small absorbance changes were observed with potential oxygen donor ligands such as acetate and benzoate in

reactions with the $[WO(H_2O)(CN)_4]^{2-}$ complex, confirming that the stability constant of the substituted complexes to be less than unity. It is further expected that the $[WO(\eta^1\text{-pic})(CN)_4]^{3-}$ complex, with the aqua ligand in $[WO(H_2O)(CN)_4]^{2-}$ substituted by the pyridine nitrogen atom, would have a very small stability constant since the $-COO^-$ group is a much stronger base (pK_a = 1.0 of the $-COO^-$ group in pic^-) compared to the pyridine nitrogen atom (pK_a = 5.52 of the protonated nitrogen of picH).

The difference in coordinating ability between the pyridine nitrogen atom and the oxygen atom of the carboxylate group is also evident from the crystal structure determinations of the $(Ph_4P)[MnN(bipy)(CN)_3]\cdot 0.5(bipy)\cdot 2H_2O$ and $(Ph_4As)_2[MnN(pic)(CN)_3]\cdot 4H_2O$ (see § 5.4 and 6.3). The Mn-O bond length *trans* to the Mn=N moiety in the $[MnN(pic)(CN)_3]^{2-}$ complex is 2.214(3) Å, whereas the Mn-N bond length *trans* to the Mn=N moiety in the $[MnN(bipy)(CN)_3]^-$ complex is 2.245(3) Å, confirming a much stronger coordination of the $-COO^-$ compared to the pyridine nitrogen of the pyridine-2-carboxylate ligand. The same tendency in bond strengths for the above-mentioned ligands was also observed in the $[WO(pic)(CN)_3]^{2-}$ [W-O = 2.171(8) Å][21] and the $[WO(bipy)(CN)_3]^-$ [W-N = 2.307(8) Å][20] complexes.

The structure determinations of the $[MX(pic)(CN)_3]^{2-}$ complexes [M = manganese(V), molybdenum(IV) and tungsten(IV); X = oxo or nitrido] mentioned above are ideal for the characterization of the stereochemical isomer formed, but cannot give any information with regard to the rate-determining step in these two step processes. As discussed above, the kinetic results of the reactions between the $[MnN(H_2O)(CN)_4]^{2-}$ and the different pyridine carboxylate ligands will be analysed with the assumption that the aqua ligand is substituted by the $-COO^-$ group first and that successive ring-closure is effected by cyano substitution of the pyridine nitrogen atom of the different pyridine carboxylate ligands in the second step of this two step process. This conclusion is made from facts obtained from various previous kinetic studies.[15,16,17]

Although the rates of the monodentate substitution reaction of the $[MnN(H_2O)(CN)_4]^{2-}$ complex could not be determined, valuable information obtained from the analogous oxo and nitrido complexes of molybdenum(IV), tungsten(IV), technetium(V), rhenium(V) and osmium(VI) can give some insight into the reaction behaviour of the

nitridocyano complexes of manganese(V). The available kinetic studies for the four $[MO(H_2O)(CN)_4]^{n-}$ [M = molybdenum(IV)[8,9], tungsten(IV)[10,11,12], technetium(V)[5] and rhenium(V)[13,14]] and the two $[MN(H_2O)(CN)_4]^{2-}$ [M = rhenium(V)[1] and osmium(VI)[2]] systems showed that the substitution of the aqua ligand proceeds most probably *via* a dissociative pathway. The most conclusive evidence is the positive volume of activation (+10.6(5) $cm^3\ mol^{-1}$) that was determined for the reaction between the $[WO(H_2O)(CN)_4]^{2-}$ complex and N_3^- anions.[11] Furthermore, the mode of distortion of the normal octahedron (i.e., the displacement of *ca.* 0.35 Å of the central metal atom towards the nitrido ligand from the plane formed by the four equatorial cyano carbon atoms in the case of $[ReN(H_2O)(CN)_4]^{2-}$ [32]) favours a dissociative pathway, since this distortion results in crowding of the complex in the probable region of attack of the entering ligand in an associative pathway. This type of distortion results in a C-M-OH_2 bond angle that is significantly smaller than the 90° for an ideal octahedron, only 80.6° in the case of $[ReN(H_2O)(CN)_4]^{2-}$. The same type of distortion was observed in the crystal structure determination of the $[MnN(CN)_4]^{2-}$ complex[30] (0.435(1) Å for the Mn^V atom), obtained from a $[MnN(H_2O)(CN)_4]^{2-}$ solution and thus, the $[MnN(H_2O)(CN)_4]^{2-}$ would have a slightly smaller distortion compared to the $[MnN(CN)_4]^{2-}$ complex. Thus, the substitution of the aqua ligand in $[MnN(H_2O)(CN)_4]^{2-}$ should also proceed *via* a dissociative mechanism.

If it is assumed that the fast reaction observed during the kinetic study of the reaction between $[WO(H_2O)(CN)_4]^{2-}$ and pic^- involves the substitution of the aqua ligand, then the forward rate for this step (0.80(8) $M^{-1}s^{-1}$)[17] is in good agreement with the literature values for the substitution of the aqua ligand by CN^-, N_3^-, NCS^- and py [k_1 = 1.15(3), 4.2(1), 2.9(1) and 6.9(4) $M^{-1}s^{-1}$, respectively] (Table 7.3 and Table 7.4).[10,11,12] This observation is based on the legitimate assumption that this anation reaction proceeds *via* a dissociative pathway. Supportive evidence for dissociative activation also stem from the fact that the equilibrium constant for the aqua substitution is very dependent on the entering ligand, while the anation rates are insensitive to the nature of the entering nucleophile (K_1 varies by a factor of 2000, whereas k_1 only varies by a factor of 5 for the ligands, CN^-, N_3^-, NCS^-, py for the $[WO(H_2O)(CN)_4]^{2-}$ complex, Table 7.3). If the slow reaction is assumed to be aqua substitution, then the 3 orders of magnitude difference between the reaction rates obtained with the mentioned monodentate ligands and the pic^- ions is difficult to explain in terms of a dissociative

pathway. The same reasoning applies to the substitution behaviour of the $[MnN(H_2O)(CN)_4]^{2-}$ complex. The rate of anation of the $[MnN(H_2O)(CN)_4]^{2-}$ complex is too fast to determine even on a 3rd generation stopped-flow spectrophotometer. However, the crystal structure determination of the $[MnN(NCS)(CN)_4]^{2-}$ complex (see § 4.3) proves that the $[MnN(H_2O)(CN)_4]^{2-}$ complex can undergo monodentate substitution reactions to form the $[MnN(L)(CN)_4]^{3-}$ substituted complexes.

It is known that the second ring-closure step is often much faster than the initial coordination of the entering ligand in aqua metal ions. However, it is anticipated that the substitution of a coordinated cyano ligand would be much more difficult than the replacement of the labile aqua ligand in this type of complexes.[17] It is expected that the cyano ligand should be more strongly bonded to the metal center compared to the aqua ligand. The relative difference in metal-ligand bond strength of the equatorial cyano ligand compared to the aqua ligand *trans* to the nitrido ligand is illustrated by the difference in bond distances for the $[MnN(CN)_5]^{3-}$ complex[29] with cyano ligands in both the four equatorial positions and *trans* to the nitrido position. The $Mn\text{-}CN_{(eq)}$ bond distance for cyano ligand (bonded in the equatorial plane) is 1.990(6) Å (average), while the $Mn\text{-}CN_{(trans)}$ bond distance (bonded trans to the nitrido ligand) is 2.243(7) Å. It is also expected that the $Mn\text{-}OH_2$ bond distance will be even longer than the $Mn\text{-}CN_{(trans)}$ bond distance. The same tendency was found for the rhenium(V) system in the $[ReN(CN)_5]^{3-}$ complex[34] with the $Re\text{-}CN_{(eq)}$ = 2.12(1) Å compared to $Re\text{-}CN_{(trans)}$ = 2.39(1) Å and the even longer $Re\text{-}OH_2$ bond distance of 2.496(7) Å in the $[ReN(H_2O)(CN)_4]^{2-}$ complex.[32] These two cases clearly illustrate the increased lability expected of the aqua ligand compared to that of the equatorially coordinated cyano ligands. Thus, it is clear that the displacement of an equatorial cyano ligand and the ring-closure by the pyridine nitrogen atom is expected to be much slower than the substitution of the aqua ligand by the carboxylate oxygen atom of the different pyridine carboxylate ligands.

It is expected that the slower second reaction would be independent of both the pH of the solution and the concentration of the entering bidentate ligand (pic^-). However, this does not seem to be the case, since the pH (Figure 7.4 and Figure 7.8) and

[34] Purcell, W.; Potgieter, I.M.; Damoense, L.J.; Leipoldt, J.G., *Transition Met. Chem.*, **1991**, *16*, 473.

ligand concentration (pic^-) (Figure 7.3, Figure 7.7, Figure 7.11 and Figure 7.14) seem to have an effect on the rate of the slower second reaction. As mentioned earlier, the rate of the first reaction was could not be determined during the course of this study due to the very fast reaction rates and the small accompanying absorbance changes. Results from the kinetic study of the reaction of the $[WO(H_2O)(CN)_4]^{2-}$ with pic^- have shown that the equilibrium constant (K_1, see reaction **C**, Scheme 7.2) for the first reaction is relatively small and in the tungsten(IV) system close to unity.[17] The results from the kinetic studies of the reactions of the $[MoO(H_2O)(CN)_4]^{2-}$ complex with 1,10-phenantroline and 2,2'-bipyridine[16] were interpreted in view of the aqua substitution being the rate determining step.[15] This stems from the fact that only one reaction was observed in both of these cases. This can be directly attributed to the low stability constant for the $[MoO(L)(CN)_4]^{n-}$ complexes, as compared to the corresponding tungsten(IV) complexes. The stability constants for the known monodentate substituted $[MO(L)(CN)_4]^{n-}$ complexes, L = CN^-, F^-, N_3^-, NCS^- ions and py, are for molybdenum(IV)[8,9]: 95(5), 12.1(9), 1.5(1), 0.2(1), 0.05(2) M^{-1} and for the tungsten(IV) complexes[10,11,12]: 1.1(1) x 10^3, 1.4(2) x 10^2, 4.8(11), 2.0(1), 0.5(1) M^{-1}. The equilibrium constants are clearly an order of magnitude smaller for the molybdenum(IV) complexes than the tungsten(IV) complexes. The same tendency for the stability constants of the monodentate substituted $[MnN(L)(CN)_4]^{n-}$ complexes is expected, since the stability constant of the $[MnN(CN)_5]^{3-}$ complex was determined as 168(20) M^{-1} during this investigation. This may also explain why only one reaction was observed for the two step reaction between the $[MnN(H_2O)(CN)_4]^{2-}$ complex and the different pyridine carboxylate ligands. Furthermore, since the anation reactions of the $[MnN(H_2O)(CN)_4]^{2-}$ complex is very fast (could not be measured), the first reaction would be difficult to observe under the reaction conditions necessary (very high concentration of the bidentate ligand) to have a significant amount formed of the $[MnN(\eta^1\text{-pic})(CN)_4]^{3-}$ (pic = different bidentate pyridine carboxylates) complexes. Thus, to date, using only the much more water soluble bidentate ligand pic^- (compared to the 1,10-phenanthroline and 2,2′-bipyridine) and employing the less reactive $[WO(H_2O)(CN)_4]^{2-}$ complex ensured the isolation of the thermodynamically unfavourable first reaction and enabled the correct analysis of the bidentate substitution reactions in these systems.[17]

Since the equilibrium constants, keeping the above-mentioned arguments in mind,

could not be determined for first fast reaction between $[MnN(H_2O)(CN)_4]^{2-}$ and the different pyridine carboxylate ligands, the forward rate constant obtained from the k_{obs} *vs.* [LL] data (LL = bidentate pyridine carboxylate ligands) is the product of the K_1k_2 term in eq. 7.5 and this term is represented as k'_1 in eq. 7.6. The forward rate constants (k'_1) for the reaction between $[MnN(H_2O)(CN)_4]^{2-}$ and different bidentate pyridine carboxylate ligands seem to compare well with the forward rate constant (k_2) of the second step found for the reaction between $[WO(H_2O)(CN)_4]^{2-}$ and pic^- ions ($1.80(8) \times 10^{-3}$ s^{-1}). The only conclusion, if any, to be made from this is that the equilibrium constants (K_1) of the first reaction seem to be near to unity, as in the case of the tungsten(IV) system. The slightly slower forward rate (k'_1) for the reaction of $[MnN(H_2O)(CN)_4]^{2-}$ and 2,4-$dipic^{2-}$ may be explained in terms of the electron withdrawing properties of the $-COO^-$ group in the *para* position on the pyridine ring. The electron withdrawing capability of $-COO^-$ group on the *para* position would make the aromatic ring less electron rich, resulting in the pyridine ring of the 2,4-$dipic^{2-}$ ligand being less nucleophilic. However, the forward reaction rates (k_1) of the pic^-, 2,3-$dipic^{2-}$ and 2,5-$dipic^{2-}$ ligands are the same within experimental error and it might be that the electron withdrawing of the $-COO^-$ group in the *meta* position of the aromatic ring in the case of the 2,3-$dipic^{2-}$ and 2,5-$dipic^{2-}$ ligands is not that significant compared to the 2,4-$dipic^{2-}$ ligand. As explained above, these substitution reactions proceed *via* a dissociative mechanism and thus, the effect of the entering nucleophile will be relatively small (relatively small influence on k_1).

The pH dependence of the second slower step can be explained as a result of the small equilibrium constant (as explained above) for the substitution of the aqua ligand. It is rather unfortunate that the pK_a values could not be determined more accurately, because of the decomposition of these substituted complexes at high pH.

The forward rate constant (k'_2) of the reaction between $[MnN(OH)(CN)_4]^{3-}$ and the different pyridine carboxylate ligands at pH 14 could not be determined successfully due to the decomposition of these complexes at the high OH^- concentration. The fast reaction between the $[MnN(OH)(CN)_4]^{3-}$ complex and pic^- ions at higher pH-values is hard to explain, since it is expected that the forward rate of these reactions will decrease with an increase in pH, as observed in the case of the tungsten(IV) system.[17] It may be due to a slightly different mode of activation for the first reaction

at high pH. It might be that the reaction at high pH proceeds *via* an interchange mechanism as well. It was found in a kinetic study of the oxygen exchange of the $[MO(OH)(CN)_4]^{m-}$ complexes that the results could only be explained successfully by an interchange or even an associative mechanism.[18]

The activation mode of the ring-closure and cyano ligand substitution step is not known at this point and further research in this regard is currently being planned. The activation enthalpy and entropy values reported in Table 7.2 are of the expected magnitude, however, since these values were determined from the forward rate constants for the overall process it may be erroneous to presume that these values may indicate towards a dissociative or an associative process for either of these two reactions. Further work, i.e. high pressure kinetics, is required for the verification of the reaction mechanism for the second reaction, since elucidation of the reaction mechanisms purely on these activation parameters has been shown to be unreliable.[35]

[35] Leipoldt, J.G.; Basson, S.S.; Roodt, A., *Advances in Inorganic Chemistry*, ed. Sykes A.G., **1993**, *40*, 241.